GA–A25579

DEVELOPMENT OF ITER-RELEVANT PLASMA CONTROL SOLUTIONS AT DIII-D

by

D.A. HUMPHREYS, M. BAKHTIARI, J. BLAIR, J.R. FERRON, Y. IN,
G.L. JACKSON, H. JHANG, R.D. JOHNSON, J.S. KIM, R.J. LAHAYE,
J.A. LEUER, B.G. PENAFLOR, E. SCHUSTER, M.L. WALKER,
H. WANG, A.S. WELANDER, D.G. WHYTE

OCTOBER 2006

GENERAL ATOMICS

DISCLAIMER

GA–A25579

DEVELOPMENT OF ITER-RELEVANT PLASMA CONTROL SOLUTIONS AT DIII-D

by

D.A. HUMPHREYS, M. BAKHTIARI,* J. BLAIR,[†] J.R. FERRON, Y. IN,[‡]
G.L. JACKSON, H. JHANG,[§] R.D. JOHNSON, J.S. KIM,[‡] R.J. LAHAYE,
J.A. LEUER, B.G. PENAFLOR, E. SCHUSTER,[†] M.L. WALKER,
H. WANG,[£] A.S. WELANDER, D.G. WHYTE*

*University of Wisconsin-Madison, Madison, Wisconsin
[†]Lehigh University, Bethlehem, Pennsylvania
[‡]Far-Tech, Inc., San Diego, California
[§]NFRC/KSTAR, Daejon, Korea
[£]ASIPP/EAST, Hefei, China

GENERAL ATOMICS PROJECT 30200
OCTOBER 2006

GENERAL ATOMICS

Abstract

The requirements of the DIII-D physics program have led to the development of many operational control results with direct relevance to ITER. These include new algorithms for robust and sustained stabilization of neoclassical tearing modes (NTM) with electron cyclotron current drive (ECCD), model-based controllers for stabilization of the resistive wall mode (RWM) in the presence of ELMs, coupled linear-nonlinear algorithms to provide good dynamic axisymmetric control while avoiding coil current limits, and adaptation of the DIII-D Plasma Control System (PCS) to operate next-generation superconducting tokamaks. Development of integrated plasma control, a systematic approach to model-based design and controller verification, has enabled successful experimental application of high reliability control algorithms requiring a minimum of machine operations time for testing and tuning. The DIII-D PCS hardware and software and its versions adapted for other devices can be connected to integrated plasma control simulations to confirm control function prior to experimental use. This capability has been important in control system implementation for tokamaks under construction and is expected to be critical for ITER.

1. Introduction

As the first operating burning plasma device, control performance requirements in ITER [1] will exceed those of present-day experiments. In addition, the ability to use operational time to empirically and iteratively improve control performance will be severely constrained by machine protection limits and availability of experimental time. Under these conditions the need for systematic model-based control design tools is critical. A longtime program of control development has produced many control solutions and an extensive set of modeling and design tools for development of controllers to support the demanding advanced tokamak (AT) mission of DIII-D [2]. Over the last decade this rich tokamak modeling environment has also been applied to many present and next-generation devices (including ITER), and in particular to operating devices that share the DIII-D PCS [3]. Section 2 describes this highly flexible environment (TokSys), its application to next-generation devices and its use in design and verification of control algorithms.

DIII-D integrated plasma control tools have been successfully applied to design and operational use of improved algorithms for suppression of NTMs through realtime tracking of q-profile evolution to maintain ECCD/island alignment following island suppression [4]. This capability will be required in order to sustain robust suppression of NTMs in ITER, which in turn will reduce disruptivity and increase the attainable plasma beta. Because the present ITER design locates the ECCD launchers at a high outboard poloidal position, current deposition will be broad and the efficiency of island suppression is expected to be correspondingly lower. In this case, alignment accuracy alone will not be sufficient to fully stabilize the mode. Modulation of gyrotron power to drive current near the O-point while

avoiding driving current near the island X-point is expected to be essential as well [5]. New PCS hardware and algorithms have been developed to accomplish the required high frequency modulation and phase alignment and to demonstrate this control action in DIII-D. Section 3 describes experimental use of q-profile tracking and development of new gyrotron modulation control in DIII-D.

The ITER poloidal field (PF) coil set is highly optimized to provide sufficient plasma shape flexibility while satisfying cost constraints. This optimization implies a significant amount of operation near coil current limits. Algorithms that can maximize the distance from these limits while maintaining good axisymmetric control will be necessary to enable robust operation of ITER equilibria. Section 4 describes a nonlinear algorithm that accomplishes this same current limit avoidance with minimal detrimental impact on shape control and has been demonstrated experimentally on DIII-D.

ITER is expected to explore the higher beta regimes that should be accessible following stabilization of the resistive wall mode (RWM). Although the algorithms required to produce such stabilization are relatively complex, the experimental time expected to be available in ITER for control optimization will be limited. Thus, controllers must be developed based on validated plasma-conductor models, and both the implementation and the expected performance must be extensively verified with simulations prior to experimental use. Section 5 describes a low order yet accurate dynamic model of the DIII-D RWM system along with control designs based on the model. Both are readily applicable to next-generation devices.

2. Integrated Plasma Control

Integrated plasma control (IPC) is a systematic approach to design and verification of controllers for tokamak operation. The approach is characterized by control designs using physics-based models validated by experimental results, confirmation of performance in the presence of system dynamics (e.g., power supply saturation), and verification of both controller implementation and performance by operating actual control software and hardware against simulations. Use of validated physics-based models is essential in order to allow high confidence extrapolation to related regimes in devices which do not yet exist or which have not produced those regimes. System-identified or database-trained models, for example, are difficult or impossible to extrapolate with confidence.

The IPC approach is realized by the GA TokSys modeling and simulation environment, now applied to and in use on many devices worldwide. TokSys, implemented in Matlab® and Simulink®, includes tools for construction of axisymmetric and nonaxisymmetric MHD control models in tokamaks, for design of relevant controllers, and for testing against nonlinear simulations. TokSys has been applied to dozens of operating devices, device designs, and next-generation devices newly started up or soon to be operating. Figure 1 shows poloidal cross-sections for a selected subset of these devices in the common representation of TokSys. Many of these devices use the DIII-D PCS. The DIII-D PCS is a highly flexible multi-cpu general realtime control environment allowing implementation of arbitrarily extremely complex algorithms. The architecture also enables connection of actual PCS hardware and software to detailed simulations to confirm correct code implementation and control performance prior to experimental use. The generality, flexibility, and extensive operational algorithms available in the DIII-D PCS have led to its adoption at fusion experiments worldwide, including MAST [6], NSTX [7], KSTAR [8], EAST [9], and PEGASUS [10]. The combination of the TokSys environment and the PCS has been used to develop and verify startup and shape control algorithms for several of these devices. Many of

the features and solutions of the DIII-D PCS satisfy requirements for and can provide useful examples in design of the ITER control system.
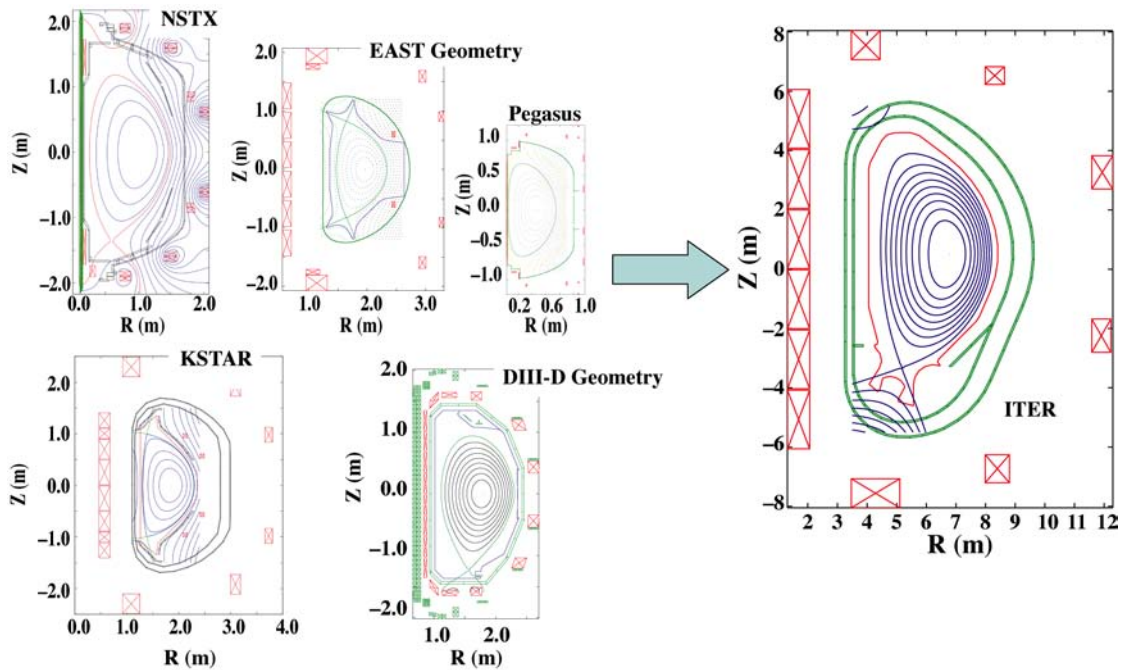

FIG. 1. Operating experimental devices and device designs for which TokSys models have been developed and integrated with a version of the DIII-D Plasma Control System.

3. Enhanced Effectiveness in NTM Suppression Using q-Surface Tracking and Modulated ECCD

IPC applied to NTM control in DIII-D has produced several search algorithms to find optimal q-surface/ECCD alignment, as well as active tracking algorithms to maintain alignment of the relevant resonant surface with the ECCD deposition spot after mode stabilization [11]. Experiments in the last two years have demonstrated robust and sustained suppression of the 3/2 and 2/1 NTM (separately) using these algorithms. Active tracking is now accomplished with realtime reconstruction of resonant q-surface geometry using motional Stark effect (MSE) measurements. The Search and Suppress algorithm performs systematic searches in ECCD/island alignment by varying major radius or toroidal field, and freezes the alignment when the mode suppression rate is sufficient, or when the island is sufficiently suppressed. Figure 2 shows results of an experiment illustrating Search and Suppress followed by active tracking with realtime q-profile reconstruction. The equilibrium reconstruction includes a rendering of the 2/1 NTM islands that grow in this discharge prior to $t = 4500$ ms. A rectangular region containing the current deposition spot is outlined in white near the $q = 2$ resonant surface and is expanded in the frame at top right. The full width at half maximum of the spot is approximately the half-width of the saturated island in this region. The gyrotrons are enabled at $t = 4500$ ms (ECH power denoted by "Pech"), and the island begins to shrink (amplitude denoted by "NTM"). Initially the island location ("Rqin") is misaligned with the ECCD ("Rec") by ~1 cm, but the search process changes the plasma major radius to bring them into alignment. Realtime reconstruction of the resonant q-surface allows this alignment to be maintained with "active tracking" even after the island is suppressed, sustaining the suppression through the end of the control phase [12]. Variations in the plasma density can change the refraction of the microwave path and with it the location of the current deposition.
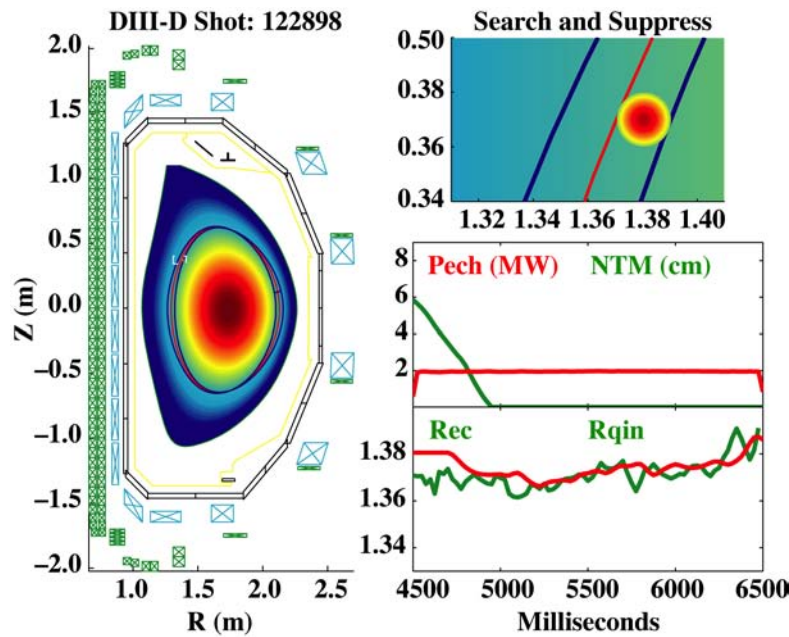
FIG. 2. Summary of an experiment illustrating use of the DIII-D Search and Suppress algorithm for NTM stabilization, followed by active tracking with realtime q-profile reconstruction.

The active tracking algorithm has been extended to correct for this refraction change based on realtime measurements of the density profile from two interferometer chords. The higher density typical of ITER operation will make this refraction effect more pronounced and will routinely require such correction.

One way to maximize NTM suppression efficiency by ECCD in ITER is to modulate the gyrotron signal to drive current near the island O-point, and turn off the power when the rotating island X-point passes through the deposition spot [5]. This requires non-zero plasma rotation, as well as the ability to detect the island frequency and phase, and to modulate the gyrotrons at relevant frequencies with specified phase. The DIII-D PCS and gyrotron control system have been upgraded to accomplish this detection and allow modulation of gyrotron power in order to demonstrate this approach. The detection algorithm assumes signals of the form $s_k(t) = A_1 \exp\{i[\phi_1(t) + \alpha_k]\} + A_2 \exp\{i[\phi_2(t) + 2\alpha_k]\}$ in each probe of a midplane-outboard toroidal array, where α_k is toroidal angle of the probe and ϕ_1, ϕ_2 are the phases of the $n = 1$ and $n = 2$ modes. Combining signals leads to a matrix equation $Pa = s$, where $a = [A_{1c}(t)\ A_{1s}(t)\ A_{2c}(t)\ A_{2s}(t)]^T$ is the set of cosine and sine coefficients and $s = [s_1\ s_2\ \cdots\ s_9]^T$. A least squares fit to the signal model at each time t is found by solving for a using the pseudo-inverse of P. The gyrotrons can be modulated at a maximum of 5 kHz with good waveform shaping. It is undesirable to reduce the rotation below this level using the new counter-NBI rotation control capability of DIII-D since such low rotation rates will likely lead to locked modes. Since the PCS is unable to generate a high-fidelity modulated square wave at such high frequencies, a dedicated computer is used to generate the signal. The PCS supplies a frequency and phase signal to this dedicated computer based on reconstruction of the mode frequency and phase.

Improved simulations for development of controllers now include island response models that represent the effect of gyrotron modulation on suppression dynamics. Figure 3 shows a simulated control scenario, which uses actual experimental data in the presence of a 2/1 NTM. Figure 3(a) shows the experimentally measured signal in a single poloidal magnetic field probe on the outboard midplane, part of the array of 11 midplane probes used to reconstruct the island size and phase. Figure 3(b) shows the corresponding detected frequency and phase of the island. When the algorithm is first enabled, an initial period (in this case 640 μs) is required to determine the frequency and phase. After that period, the frequency is updated every 640 μs while the phase (based on that frequency value) is updated

continuously. Figure 3(c) shows the resulting signal generated by the dedicated gyrotron modulation computer, well-synchronized with the island amplitude.
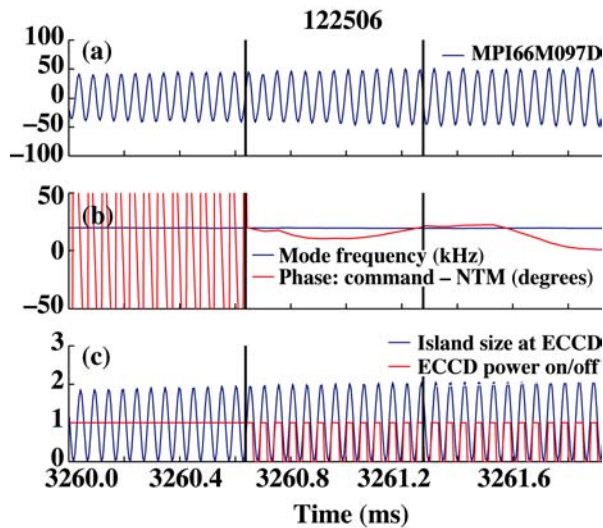

FIG. 3. *Simulation based on experimental NTM data illustrating island frequency and phase detection for gyrotron modulation in the DIII-D PCS.*
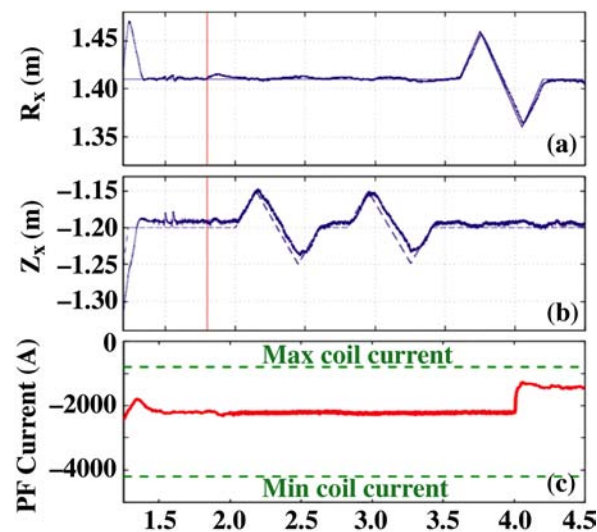

FIG. 4. *Summary of model-based multivariable boundary control in DIII-D acting in concert with feedforward current trajectories adjusted in realtime to maximize distance from coil current limits.*

The implementation of this control scheme in the PCS calculates and commands the different phases required by multiple gyrotron launchers located at different toroidal angles.

4. Experimental Demonstration of Nonlinear Shape and Coil Current Control Algorithms

Good dynamic regulation of the magnetic configuration, including boundary, divertor strikepoints, and location of internal flux surfaces, must be maintained in DIII-D to an accuracy of several millimeters, even in the presence of transient perturbations such as ELMs and sawteeth, over a wide range of shapes and profiles [13]. Axisymmetric control demands in ITER will be even more restrictive, corresponding to shaping and configuration control accuracies on the order of 5-10 times those required in DIII-D (as a fraction of minor radius). Model-based multivariable control design methods applied to DIII-D allow incorporation of performance requirements in the design process. For ITER, such approaches can provide optimized control for best use of actuators whose capabilities are limited by cost constraints.

The DIII-D "isoflux" shape control system regulates the flux at various control points located around the plasma boundary to be the same as the flux at the X-point(s) or a selected wall limited point [14]. In order to make efficient use of power supply capabilities under this scheme, DIII-D discharges often produce PF current evolutions that approach supply limits. Multivariable model-based controllers demonstrated in DIII-D (and selected as the approach for ITER axisymmetric control) seek to drive boundary errors to zero, often at the expense of attempting to exceed power supply limits. A nonlinear algorithm is required to prevent this while still maintaining acceptable control performance. Figure 4 shows a DIII-D experimental demonstration of linear model-based multivariable controllers functioning in concert with a nonlinear algorithm to maximize distance from coil current limits while maintaining good shape and X-point control. The algorithm calculates dynamically varying feedforward current trajectories for all coils, based on a linear plasma response model, in order to balance these

competing needs. This approach also provides "headroom" for coil current excursions in response to transient off-normal events. Figure 4 shows the X-point radial and vertical positions under programmed variation using a model-based controller, demonstrating good dynamic control of individual shape quantities with feedforward current trajectories.

The PF coil current shown in Fig. 4(c) requires updating by the current trajectory algorithm in the case of the R_x variation, but not for the programmed Z_x change.

Such a linear-nonlinear control system will be essential for ITER in order to provide good control near tightly constrained operating limits throughout a long pulse discharge.

5. Resistive Wall Mode Control Based on Finite Element Eigenmode Models

Robustness of RWM stabilization has been observed to be degraded by the effects of ELMs on control response and to be sensitive to the instantaneous growth rate of the mode [15,16]. New plasma-conductor models have been developed based on an eigenmode representation of the DIII-D passive

FIG. 5. Finite element mesh represent-ation of DIII-D for calculation of coupling among vessel eigenmodes, active coils, and plasma surface current mode. (b) Surface current patterns (1-3).

structure, allowing low-order model-based controllers to be designed for robustness to growth rate variation and ELMs. The model description used in the TokSys RWM modules consists of a first order matrix circuit description:

$$M_{ss}\dot{I}_s + R_{ss}I_s + M_{sp}C_{pp}M_{ps}\dot{I}_s = V_s \quad , \tag{1}$$

where I_s and V_s denote currents and voltages in stabilizing conductors, including both vessel wall and active control coils. C_{pp} is a scalar coupling coefficient between the modal perturbed surface current K_p and the plasma surface flux, ψ_p. Defined by $K_p = C_{pp}\psi_p = C_{pp}(M_{ps}I_s)$, C_{pp} completely describes the energy source driving the instability. Vessel wall current states can be described by surface current eigenmodes, derived by solving an eigenvalue equation of the form [16]

$$\nabla_s \cdot \left[\frac{n}{\Delta}(\vec{\nabla}\nu)^2 \nabla_s K_m \right] = -(\vec{\nabla}\nu)^2 \lambda_m K_m \quad , \tag{2}$$

where $K_m(l,\phi) = \kappa_m(l)e^{-in\phi}$ and the surface Laplacian is given by $\nabla_s = \hat{l}(1/R)(\partial/\partial l)R + \hat{\phi}(in/R)$ in the (radial dimension, poloidal length, toroidal angle) coordinate system (ν, l, ϕ). The eigenvalues (λ_m) play the role of surface resistors with units of resistivity/length [16]. The eigensystem [Eq. (2)] is solved and the mutual inductance couplings of [Eq. (1)] are derived using the finite element representation shown in Fig. 5.
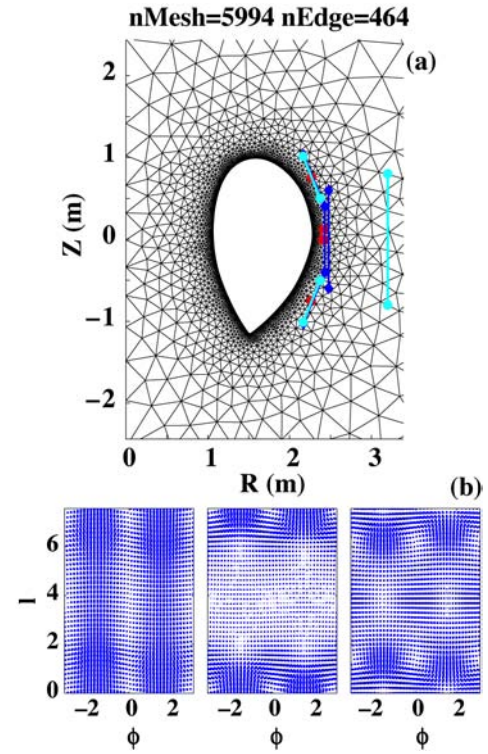
Principal actuators for RWM control in DIII-D are a set of six picture-frame, in-vessel "I-coils" evenly spaced toroidally above the outboard-midplane and connected in $n = 1$ pairs, and six identical coils connected in $n = 1$ pairs below the outboard midplane. One control approach is to make the control voltages applied to each pair of the set of 12 I-coils depend on matched filter estimates of the RWM mode amplitude from magnetic diagnostics [17]. Figure 6 shows contours of stability for various mode growth rates using "diagonal" PD controllers in the space of proportional and derivative gains, G_p and G_d. Figure 6(a) shows that for sufficiently low growth rate (10 rad/s; black contour) a large stable gain space exists, but the stable region shrinks rapidly as growth rate increases (e.g., 1000 rad/s; red contour). Figure 6(b) magnifies the stable region corresponding to 1000 rad/s, showing the stable gain spaces continuing to shrink as the growth rate increases to 4000 rad/s. At a growth rate of ~ 4100 rad/s, the stable space vanishes, and the mode cannot be stabilized beyond this value with such a PD controller. To reach the ideal limit in DIII-D is predicted by the VALEN code to require stabilizing growth rates on the order of 5000 rad/s [18]. A single pair of PD gains (e.g., G_p = 20,000 and G_d = 13) can stabilize this entire range of growth rates, possibly avoiding the need for gain scheduling. Realistic power supply dynamics and the effects of computational delays have been taken into account in this analysis.
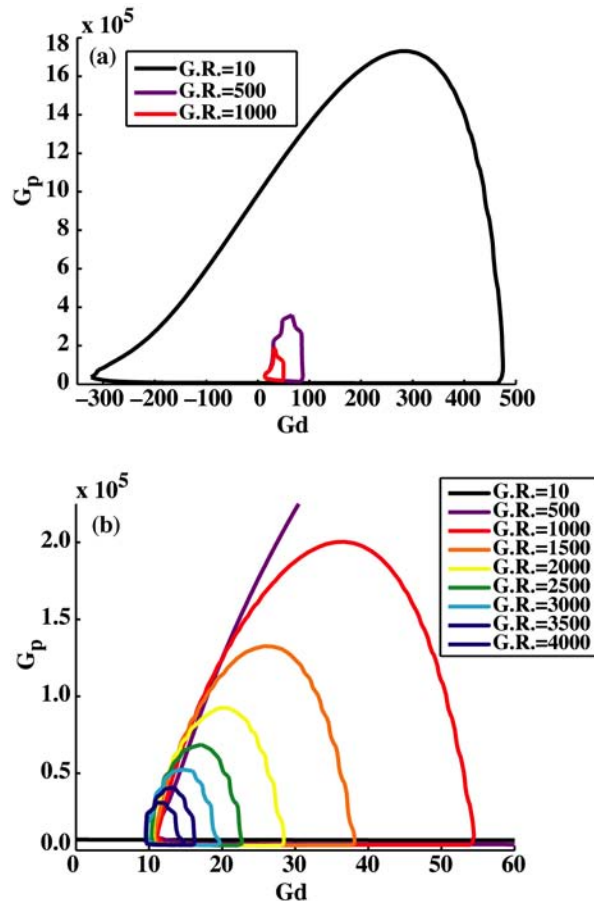

FIG. 6. Contours of stable gain spaces for varying RWM growth rates. The interior of each contour corresponds to a closed-loop stabilized RWM.

In contrast with the PD controller, linear quadratic gaussian (LQG) controllers have also been designed and analyzed. In this case, a single choice of gains are found to allow stabilization of higher growth rates, up to 6200 rad/s. Unlike the diagonal PD controller, an LQG controller

fully populates the gain matrix and allows broader dynamic range of control response, improving performance over simple proportional-derivative (PD) controllers.

6. Summary and Conclusions

Owing largely to its superconducting PF coils distant from the plasma surface and the constraints of its burning plasma mission, ITER demands completely new control algorithms, as well as higher accuracy and more reliable control than required on present-day experiments. Integrated plasma control, a systematic method for designing and confirming high-confidence control algorithms, is particularly important for such a device. DIII-D model-based multivariable linear shape and stability control algorithms coupled with a unique nonlinear feedforward current trajectory algorithm offer a solution to the key ITER problem of operation near coil current limits. Model-based and simulation-verified NTM suppression algorithms using modulated ECCD to maximize current drive effectiveness in DIII-D demonstrates this critical set of capabilities for eventual ITER application. New approaches to RWM system modeling and resulting model-based controllers for DIII-D demonstrate the usefulness of the IPC approach for global MHD control and provides a path to transfer RWM control results from DIII-D to ITER.

References

[1]　AYMAR, R., et al., Nucl. Fusion **41** (2001) 1301.
[2]　FERRON, J.R., et al., Plasma Physics and Controlled Fusion (Proc. 29th Conf. Montreux, 2002), EPS, Paris vol. 26B, P1.060.
[3]　PENAFLOR, B.G., et al., Fusion Engin. Design **71** (2004) 47.
[4]　HUMPHREYS, D.A., et al., Phys. Plasmas **13** (2006) 56113.
[5]　La HAYE, R.J., et al., Nucl. Fusion **46** (2006) 451.
[6]　LLOYD, B., et al., Fusion Energy (Proc. 19th Conf. Lyon, 2002) IAEA, Vienna, OV/2-3.
[7]　SYNAKOWSKI, E.J., Fusion Energy (Proc. 19th Conf. Lyon, 2002) IAEA, Vienna, OV/2-2.
[8]　KWON, M., BAK, J., LEE, G.-S., Fusion Sci. Technol. **42** (2002) 167.
[9]　WAN, Y.X., et al., Fusion Energy (Proc. 19th Conf. Lyon, 2002) IAEA, Vienna, FT/P2-03.
[10]　GARSTKA, G.D., et al., Nucl. Fusion **46** (2006) S603-S612.
[11]　La HAYE, R.J., et al., Phys. Plasmas **9** (2002) 2051.
[12]　La HAYE, R.J., et al., Nucl. Fusion **45** (2005) L37.
[13]　WALKER, M.L., et al., Fusion Sci. Technol. **47** (2005) 790.
[14]　WALKER, M.L., et al., Decision and Control (Proc. 36th Conf. San Diego, 1997) IEEE, Piscataway (1998) 3703.
[15]　FRANSSON, C.M., et al., Phys. Plasmas **10** (2003) 3961.
[16]　IN, Y. et al., Phys. Plasmas **13** (2006) 062512.
[17]　EDGELL, D.H, et al., Rev. Sci. Instrum. **73** (2002) 1761.
[18]　STRAIT, E.J., et al., Phys. Plasmas **11** (2004) 2497.